An inspection system for pharmaceutical glass tubes

Pierfrancesco Foglia, Cosimo Antonio Prete
Dipartimento di Ingegneria dell'Informazione
Università di Pisa
Via Diotisalvi 2, Pisa
ITALY
foglia,prete@iet.unipi.it

Michele Zanda
R&D
ION Trading
Via San Martino 54, Pisa
ITALY
michele.zanda@iontrading.com

Abstract: Syringes, vials and carpules for pharmaceutical products are usually made of borosilicate glass. Such containers are made by glass converting companies starting from single glass tubes. These glass containers can suffer from inclusions, air bubbles, stones, scratches and others issues, that can cause subsequent problems like product contamination with glass particulate or cracks in the glass. In recent years, more than 100 million units of drugs packaged in vials or syringes have been withdrawn from the market. As a consequence pharmaceutical companies are demanding an increased delivery of high quality products to manufacturers of glass containers and therefore of glass tubes. An automatic, vision based, quality inspection system can be devoted to perform such task, but specific process features requires the introduction of ad-hoc solutions: in the production lines tubes significantly vibrate and rotate, and the cylindrical surface of the tube needs to be inspected at 360 degrees. This paper presents the design, the development and the experimental evaluation of a vision system to control the quality of glass tubes, highlighting the specific solutions developed to manage vibrations and rotations, obtaining a 360 degree inspection. The system has been designed and tested in a real facility, and proved effective in identifying defects and impurities in the order of tens of microns.

Keywords: Inspection systems, glass tube manufacturing, quality check, machine vision systems, image processing algorithms, 360 degree Inspection.

1 Introduction

Glass tubes, that must be later converted into pharmaceutical containers such as vials, syringes and carpules, are historically been made of borosilicate glass, which is widely considered to be the most traditional and cost-effective option for a parenteral drug container or delivery system [1], [2]. Such kind of glass has historically been the preferred material for pharmaceutical packaging, but glass can present problems like particles (inclusion), air bubbles (air lines), or flexible fragments called lamellae, and these defects in glass tubes can cause subsequent problems and pharmaceutical recalls [3][4][5][6][7][8]. In recent years, more than 20 product recalls have been associated with glass issues, and over 100 million units of drugs packaged in vials or syringes have been withdrawn from the market [9][10][11]. As a consequence, it is important for pharmaceutical glass manufacturers to check the quality of the produced tubes, with the aims to deliver tubes with defects not influencing the final quality of the product. Such quality check can not be performed by humans, due to the process speed, the high quality requirements and safety concerns (high glass temperature and environmental considerations), so that an automatic inspection system is required, able to recognize defects that are relevant for the specific use of the tube. This inspection system can be realized via machine vision systems as the glass does not presents patterns, it is monochrome and translucent, and glass defects can be detected according to grey levels changing using image processing algorithms [12]. Anyway, an accurate design of the system must be performed, as, due to the production process, the tubes rotate and vibrate, and they must be inspected at 360 degrees.

This paper presents the design and development of a vision system for the quality control of pharmaceutical glass tubes, and describes the solutions developed to solve the issues posed by tubes rotation and vibration, and the need to perform inspection with 360 degrees. In particular, for what concern the image acquisition subsystem, a highly uniform illuminator working in saturation has been adopted. At software level, images were segmented

and the borders of the tube, identifying the Region of Interest (ROI) to which apply further elaborations, were individuated by searching for local minima over a threshold. The need to inspect the tube at 360° was solved with a multi-camera system and a specific algorithm that follows defects that span over multiple images. Finally, the images coming from the three cameras are analyzed and defects identified in real time with a parallel software architecture, by employing circular buffers and synchronizations to manage the parallelism in the data coming from the cameras. A multi-core architecture has permitted to concentrate in a single machine tasks previously performed in distributed architectures [12]. The proposed inspection system has been adopted by a glass tube manufacturer, and is currently being used in two production lines.

The paper is structured as follows. Section 2 introduces glass tube production, the requirements for an inspection system, and the specific issues that must be solved to satisfy such requirements. Section 3 described the overall hardware and software architecture of the systems, and presents the specific algorithms developed. Section 4 reports the achieved results in the inspection accuracy, and conclusions are given in the last section.

2 Background

2.1 Glass tube production

In the production of glass tubes, the first stage is the collection of raw materials, mainly silica sands (SiO2), and their storage in vertical silos. Silica sands are moved into a furnace where they are heated at around 1500°C to melt it in uniform manner. Then, the melted silica leaks onto a rotating mandrel that shapes the glass into a glass tube (Fig.1). The mandrel rotates to ease the forming of a circular shape in the glass, and it also blows air inside the tube with the same purpose. Rotation speed and air blowing are dynamic parameters that can be controlled by supervisors. After the mandrel, the tube undergoes a cooling and solidification phase that lasts around 50 meters (fig. 1). At the end of the cooling phase the tube is pulled by a drawing caterpillar (Drawing Machine in fig. 1).

After the drawing caterpillar, the continuous glass tube is highly solid and is cut into single tubes. After the cutting, the ends of single tubes are heated again to make them more robust (soft annealing): they are more fragile than the rest of the tube because they underwent the cutting stress. Finally, single tubes are put together, packaged, and stored in the warehouse. From the warehouse, tubes are sent to glass converters: converters transform single glass tubes in carpules, syringes, and vials for the pharmaceutical industry.

Due to the increasing quality requirements in the production system, and due to the behaviors of the process that does not permit human inspection, an automated control quality system can be introduced in the production line. To simplify the design of such system, the idea is to exploit glass movement to perform inspection; as a consequence the inspection system is introduced before the Drawing Machine. After the Cutting machine, a Discarding machine is placed, and the discarding decision is taken by the inspection system. The inspection system can be realized via machine vision systems thanks to the glass properties that permit to adapt, as inspection principle, the grey levels changing induced by glass defects, that can be detected using image processing techniques [12].

2.2 Requirements and issues in the design of the inspection system

2.2.1 Requirements of the inspection system

Among all the defects that can be present in glass tubes for pharmaceutical containers, the hardest and the most critical to find are represented by air bubbles. Air bubbles are the smallest defects that can be present: in the furnace and before the mandrel air bubbles can form in the glass walls, then the tube is pulled by the Drawing Machine, and the air bubbles elongate becoming long air lines with a little section. Given the structure of elongated air lines, that due to vibration and rotation change their thickness, achieving a high orthogonal resolution with respect to the tube movement is much more important than a longitudinal ones. In particular, glass converting companies are demanding inspection systems able to identify and discard tubes with defects with orthogonal section in the order of tens of microns. As a consequence, it is considered acceptable that a vision system identifies defects with orthogonal section larger than 15 microns, and with a longitudinal resolution of 0.5 mm.

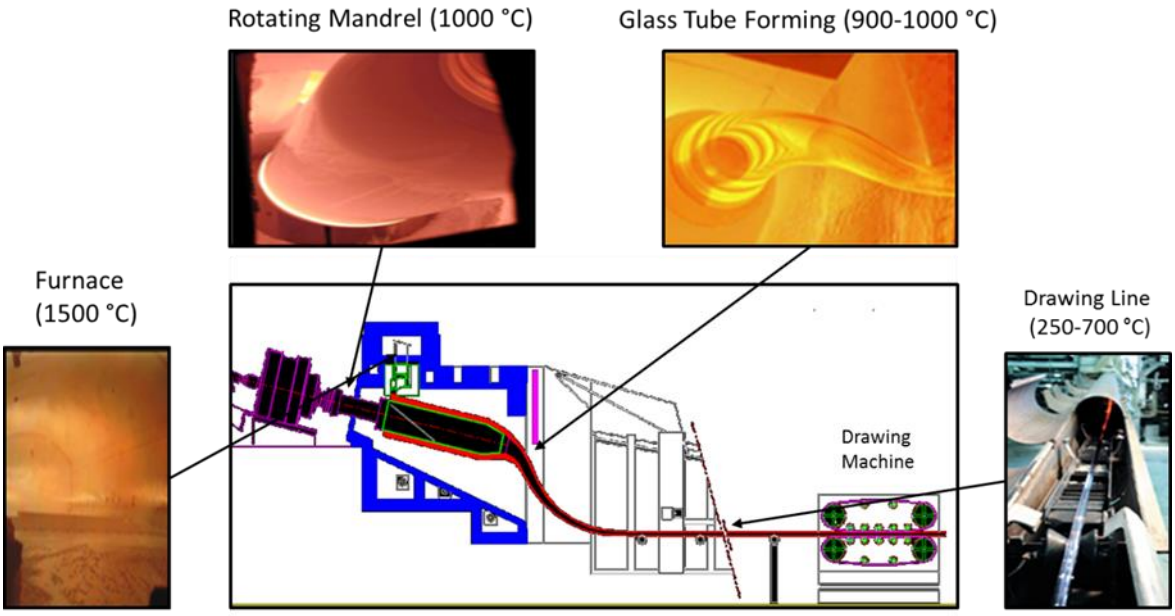

Figure 1: A scheme depicting the process of glass tube formation. A Cutting and Discarding Machine is located after the Drawing Machine (not shown in the figure).

2.2.2 Issues in the design of the inspection system

Machine vision systems are more and more adopted in manufacturing industries, especially in appearance quality control, and they have been deployed with success in a variety of fields [14], [15], [16], [17], [18], [19], [20], [21]. They have been also used in glass manufacture [12], [22], but in our case, due to peculiarity of the inspection task, there are a set of issues that do not permit to full apply standard techniques.

As the tube is pulled by the Drawing Machine for more than 50 meters, it significantly vibrates, and issues arise from having an object under inspection that vibrates. This affects both the hardware and software design of the inspection system. Vision systems that inspect objects that do not vibrate often subtract the background in the images to highlight the features of interest. The background can be considered as recurring data that must not be inspected by vision algorithms. Background subtraction, also referred as shading correction or compensation if the constant data is due to lightning, has been applied with success to inspect float glass [12], and in other application domains [23], [24], [25], [26]. In our case, the glass tube acts as a sort of double lens and vibrates significantly, so shading correction is unfeasible, and the illumination must be provided by a highly uniform illuminator to limit the need of shading correction.
A second problem derived from a vibrating object regards the need to inspect the tube with fast scans and high magnifications as very small defects must be identified. Such a combination of settings results in having a scarce light power on the sensors. Having the same problem of scarce light power, Campoy et al. [17] increase the illumination of the object under inspection through Time Delay Integration (TDI) cameras: TDI cameras accumulate exposure times on a line of sensors with multiple-line scans. Such a method can only be applied when the object under inspection does not vibrate, otherwise that summation causes an increase of noise higher than the increase of illumination, so TDI cameras cannot be adopted in our case.
To compensate vibrations, [27] utilizes hardware techniques in an automated vision system to check pressworks quality. In particular, they utilize an 11KHZ line camera and they exploit subtraction from a reference image to investigate defects. In our case, although utilizing an 8Khz camera, the effects of the movement, apart shading correction solved via illuminator, are not masked, and must be compensated with software techniques (Section 3.3.1).

Further problems derive from the need to inspect the rotating object at 360 degrees. The section of the continuous glass tube must be inspected from multiple points of view (i.e. with more than one camera), with no opportunity of rotating the tube (being continuous), and then images or defects must be merged to derive relevant metrics of quality (Section 3.2.3). A complication derives from the fact that parts of the same defect can be on different

images, and such images can be generated by the same or by different cameras. For many of the systems presented in literature (e.g. [27] for checking the presswork quality), the data acquired in a single image include the whole workpiece, so there is no need of data fusion techniques. Systems that utilize multiple cameras are described in [12] and [28]. In [12], in a vision system for defect inspection in float glass fabrication, they meanly deal with bubble and lards, that can be identified without algorithm that elaborate multiple image. They utilize multiple cameras, but image processing algorithms are applied to the stream produced by a single camera, and only the results of the classification are sent to a server that manages historical data. In [28], an inspection system for defects assessment in satin glass is presented. They utilize two cameras and they apply a mosaicking algorithm to restores the image of the whole sheet starting from the partial images obtained with different cameras and in different sampling instants, in a production process at the speed of 34 mm/s. Anyway, they work with finite size workpieces, so restoring the image of the sheet is possible, differently from our case, in which we have to deal with a continuous flowing tube.

The last problem concerns the calculation of the tube speed, that is required to calculate the defects length and to locate the defects to a specific tube. The standard approach to derive the speed of the object under inspection is the adoption of an encoder to extract the true forward movement [20], [12], [29], but in our case the glass tube slide on its supports and encoders are useless. Hence, the tube speed, needed to calculate defects length, must be derived from the tube Drawing Machine depicted in Fig. 1 (calculations shown in the next section).

3 The inspection system

The proposed inspection system has the scheme of Fig. 2-a, and it follows the general schema adopted for such systems [12]-[21], [29]. It is constituted by the Image Acquisition Subsystem and the Host Computer. The image Acquisition Subsystem is devoted to the acquisition of the digitalized images; key components of such system are a LED based illuminator, a CCD camera and the frame grabber, that converts the pixels coming from the camera in digitalized images. As shown in Fig. 2-b, we utilize 3 cameras with related illuminators and frame grabbers, as we need a 360 degrees inspection of the tube, and a single camera can inspect two portions of the tube with a global angle lower than 180 degrees. The Host Computer performs the task of image pre-processing [29], and in particular the identification of the Region of Interest (ROI) of the acquired image; the task of defects detection among different images and classification, and takes the discard decision, communicating it to a Cutting and Discarding Machine. The discarding decision is taken based on defects classification, but also on process parameters that operators can set up via a Graphical User Interface (GUI). Such GUI is utilized also to visualize on-going statistics on defects detections and discard decisions. Besides, a communication link is established, via a network connection [13], with the Quality and Order Management departments, to further set-up process parameters and exchange process data.
Thanks to the increase in performance with technology advances, the Host Computer is based on a single quad-core processor, that is devoted to performs all the functionalities, differently from [12] where a distributed architecture is proposed, with a single PC devoted to the elaboration of data from a single frame grabber, and a PC devoted to performs actuation and GUI management.

In the following, we describe how the requirements of section 2.3 determine system settings, then we present the design of the Image Acquisition Subsystem, the main software algorithms designed and implemented in the Host Computer and the deployed software architecture.

3.1 Translating requirements into specifications

The proposed vision system inspects a glass tube that moves continuously and that can be inspected from a fixed line camera [29]. A line scan camera has a single array of sensors, and a 2D image is built by collecting sequential line scans.
Each sensor in the line array of a line-scan camera covers a virtual rectangle on the glass tube (Fig. 3). The virtual rectangle inspected by a single sensor has a dimension in the orthogonal direction of the tube that can be derived from sensor size and optical magnification (formula 1), and the dimension in the longitudinal direction that can be calculated from tube speed and sensor exposure time (formula 2):

$$orthogonal\_resolution = sensor\_size \times magnification \quad (1)$$

$$longitudinal\_resolution \approx tube\_speed \times exposure\_time \quad (2)$$

The area of the virtual rectangle covered by one sensor is used to derive the sizes of the defects

observed in the images. The virtual rectangle represents a pixel in the frame.

To evaluate the longitudinal resolution, the tube speed is needed. In similar systems, usually an encoder is devoted to such measurement, but in our case, this is not possible as the tubes slide on its supports. Anyway, we can derive tube speed according to the following consideration on the production process of glass tubes: a quasi-solid glass tube goes out of the mandrel (Fig. 1) at a speed that depends on the tube caliber. The quantity of melted glass coming out of the furnace is kept constant to optimize the heating costs of the furnace, so the tube runs at different speeds depending on the quantity of glass per tube section. A tube with a small and thin caliber (e.g.: for syringes) runs faster than a tube with a large and thick caliber (e.g.: for vials). At production time, the tube speed is controlled by the Drawing Machine than sends command to the Cutting and Discarding Machine to have a single tube of an assigned length, so that tube speed can be calculated with the formula:

$$tube\_speed\ (m/s) = tube\_cuts\_per\_second\ (Hz) \times single\_tube\_length\ (m) \quad (3)$$

where *tube_speed* is within the range 0.5 ÷ 4 m/s.

Both the *tube_cuts_per_second* and the *single_tube_length* are furnished by the Drawing Machine to the Host Computer (Fig. 2-a), and theyare utilized to derive the sizes of the defects in the images.

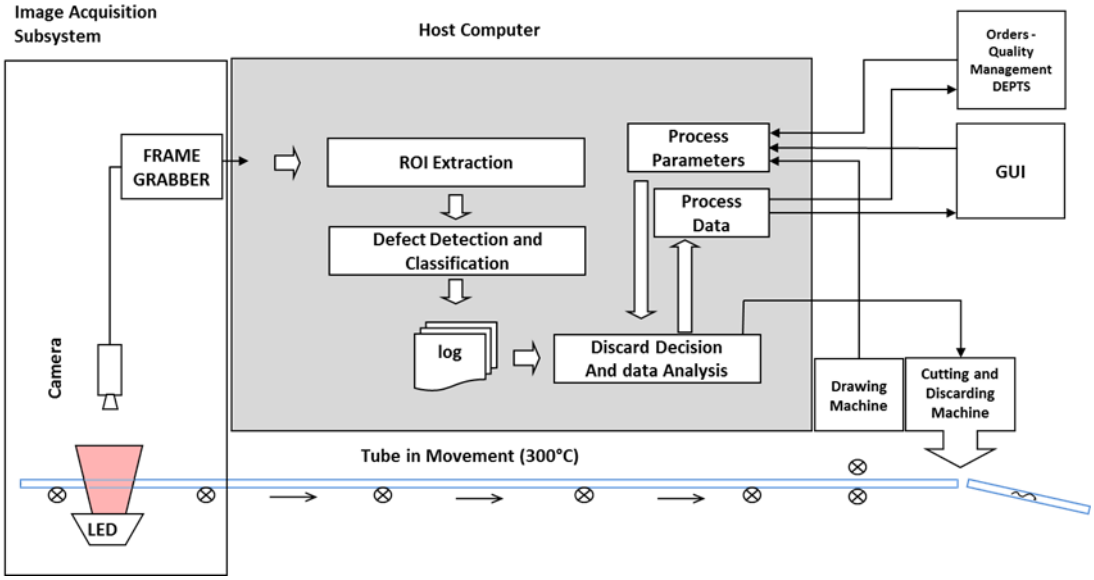

(a)

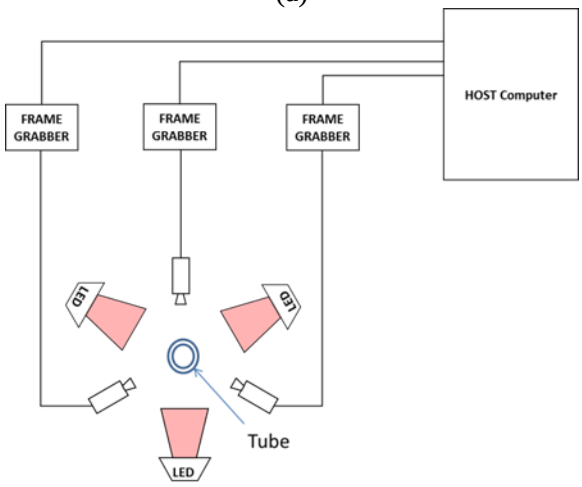

(b)

Figure 2: Architecture of the proposed inspection system (a) and layout of the cameras and the illumination system (b).

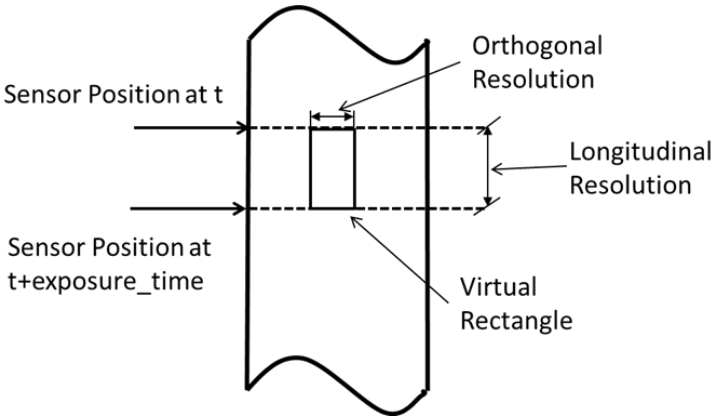

Figure 3: Each sensor in the camera covers a virtual rectangle on the image, according to formulas (2) and (3). In the next figures, the virtual rectangle will be visualized as a square.

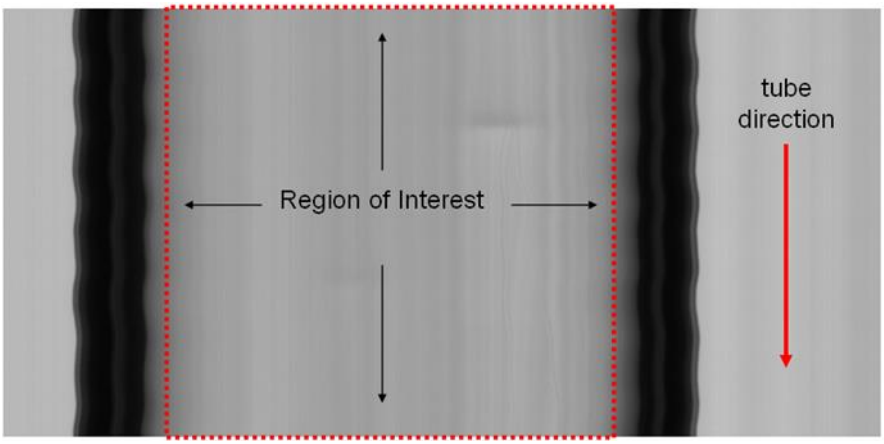

Figure 4: Image taken by one of the line-scan cameras. The array of CCD sensors in the linescan camera is orthogonal to the tube direction. The Region of Interest is also highlighted. It represents the portion of the image which is further analyzed for detecting defects.

3.2. Design of the Images Acquisition Subsystem

The quality of the acquired images plays a vital role in simplifying an inspection problem, and such quality is drastically affected by the type and level of illumination [29].

At design time, the system to inspect the glass tube could have several lighting setups: bright field, dark field, back lighting, diffuse light, or coaxial illumination, explained in detail by Pernkopfa and O'Lear [30]. After initial tests, and also replicating how experts look at the single glass tubes, we had the best performances with a back lighting system (Fig. 2). The inspection system is located before the Drawing Machine and the Cutting and Discarding machine (Fig. 1), and this means that it inspects the tube when it still continuous, not yet cut into single tubes. With backlighting, the illuminator must provide a highly uniform line of light, so that defects can be identified by light modifications. Besides, we choose a high power source of illumination, so that sensors work, with no defect, in saturation, and little variations in the light power determines no effects on the sensors acquired value.

Also the optical system and its setting are critical for the overall quality of the system. The continuous glass tube is hot and vibrates, so the inspection components cannot be positioned close to the tube. In addition, the tube has two sides, and both sides must be in focus, so also the depth field of the lens has to be considered. For these reasons, the optical lens must work in telescopic mode. In such mode, cameras can inspect an object with a maximum magnification of 1:1, the highest possible for telescopes, to have maximum resolution in the images. A high magnification implies having low depth field and increased lens aberrations. Among the tested magnifications, the best trade-off between high resolution, acceptable depth field, aberrations, and our resolution requirements, is, 1:1.5, which means, for instance, that 10μm of a sensor map onto 15μm of the image.

Having chosen optics with magnification 1:1.5, and having a requirement to inspect defects with an orthogonal resolution of 15μm, we can have sensor

in the line-scan camera with size of 10µm. For these reasons, we adopted 2k CCDs cameras, with CCDs size of 10µm. Matching the system requirements, in order to have a longitudinal resolution at maximum tube speed (4m/s) of 0.5mm, cameras must scan with a frequency of 8KHz (that corresponds to a period of 125µs per scan). With these settings, the system resolution in the orthogonal direction of the tube is always 15 µm because sensors size is 10x10µm and the optical magnification is 1:1.5. Conversely, in the longitudinal direction, each CCD sensor covers a length equal to *tube_speed* (m/s) x 125 x 10-6 s. To sum up, this setting meets the resolution requirements, given in section 2.3.1, in the two dimensions:

orthogonal resolution (1)= 10µm x 1.5 = 15µm
longitudinal resolution (2)= 4m/s x 125 x 10-6 s = 0.5 mm.

As the tube flows, the line-scan camera takes linear photos of different sections of the tube that are then combined in 2D images (fig. 4) by a frame grabber in a time interval. The inspection system has three axes of observation each with a line scan camera, and these axes virtually intersect at tube center with angles of 120° (Fig 2-b). A camera has blind areas of inspection because of the tube borders curvature (visible in Fig. 4), so a configuration with three axes is needed to inspect the whole tube circumference.
The line scan frequency (8KHz) also imposes a constraint on the maximum time to analyze an image: in our design images are made of 1000 lines, so in a time interval all the three images coming from the three cameras must be analyzed in less than 125ms (125µs x 1000).
The adoption of line-scan cameras permits to have simpler illuminators, line-based as well, and reduces aberrations caused by the lenses as the sensor spans a fraction of the lens. The illuminators in backlight configuration are LED based for their durability and uniformity, with illuminance of 1.6 Million Lux, set at red wavelength (~630nm) because at this wavelength the sensors have the higher sensibility. Clearly, with greyscale cameras, light color is irrelevant for the inspection purposes, but it is important to have high illumination because cameras have short acquisition time (125µs) and work at high magnification. Cameras transfer the line scans to frame grabbers through Camera-Link cables.

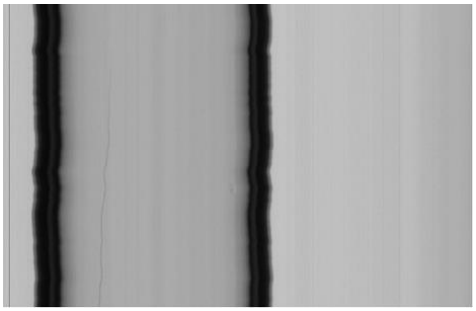

(a)

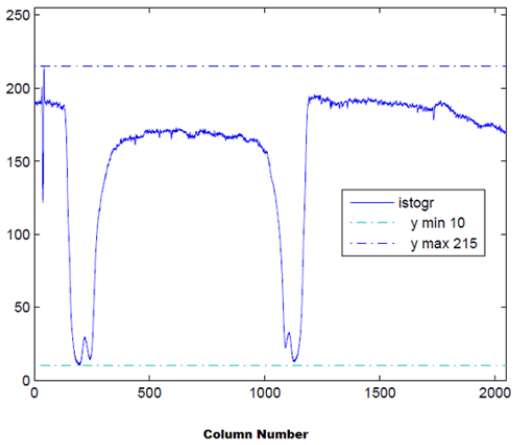

(b)

Fig. 5: (a) Image taken by a line scan camera: due to the oscillatory movement of the tube, the borders of the tube are not linear, but present an oscillatory behavior. (b) Column value histogram of image (a) averaged on all the lines of the image. There are local minima in correspondence of the inner and outer borders of the tube, while the image inside the tube presents lower values of the average with respect to the outside.

Figure 6: Effects of the movement of the tube on the acquired image.

Algorithm 1:
For each sub-image in the image {
centre=width/2;
NUM_BORDER=0;
INT_BORDER_LEFT = EXT_BORDER_LEFT = 0;
INT_BORDER_RIGTH = EXT_BORDER_RIGTH = width;
$I_{avg}(y) = \sum_{x=0}^{numline-1} \frac{I(x,y)}{numline}$;
$\overline{I_{avg}} = \sum_{y=0}^{width-1} \frac{I_{avg}(y)}{width}$;
$LEFTMIN = MIN_{y=centre}^{0} \left(I_{avg}(y)\right)$;
$YMINLEFT = y|\, I_{avg}(y) = LEFTMIN$;
If ($LEFTMIN <$ *TrueBorder_Threshold) {*
EXT_BORDER_LEFT = first value of y, with y varying from $YMINLEFT$ *to 0, for which* $I_{avg}(y) > \overline{I_{avg}}$;
INT_BORDER_LEFT = first value of y, with y varying from $YMINLEFT$ *to center, for which* $I_{avg}(y) > \overline{I_{avg}}$ - *Threshold1;*
NUM_BORDER++;
}
$RIGHTMIN = MIN_{y=centre}^{width-1} \left(I_{avg}(y)\right)$;
$YMINRIGTH = y|\, I_{avg}(y) = RIGHTMIN$;
If ($RIGHTMIN <$ *TrueBorder_Threshold) {*
EXT_BORDER_RIGTH = first value of y, with y varying from $YMINRIGTH$ *to* $width - 1$, *for which* $I_{avg}(y) > \overline{I_{avg}}$;
INT_BORDER_RITGH = first value of y, with y varying from $YMINRIGTH$ *to center, for which* $I_{avg}(y) > \overline{I_{avg}} - Threshold1$;
NUM_BORDER++;
}

<ROI> = Columns from INT_BORDER_LEFT to INT_BORDER_RIGTH;

}

Figure 7: Algorithm for the detection of the ROI.

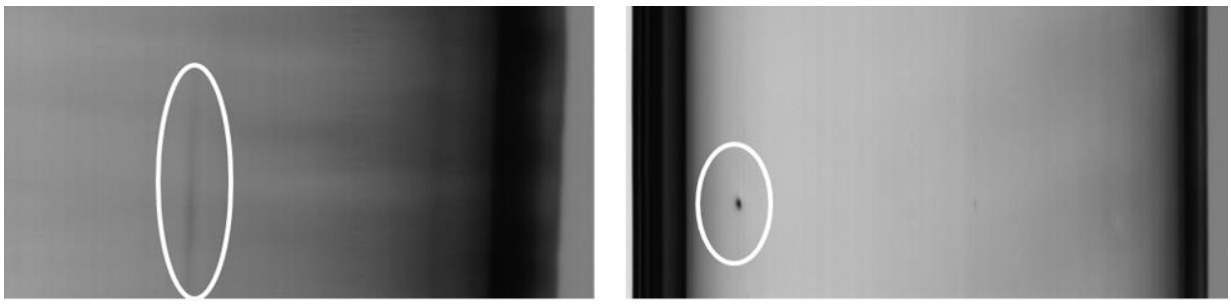

(a) (b)

Figure 8: Samples of defects detected by the line-scan cameras: an air line (a) and a knot inclusion (b). As virtual rectangle are represented as square, the real size of the defect is different from what is depicted in the image.

3.3. Software algorithms implemented in the Host Computer

3.3.1. Identification of the ROI

The first operation performed on the acquired images is the identification of the Region of Interest (ROI), i.e. the portion of image to be analyzed (Fig. 4). The algorithm starts from the consideration that (Fig. 5), for a typical image, the average value of the columns that constitute the image presents 4 local minima, in correspondence of the external and internal left margins, and the external and internal right margins of the borders of the tube. Such minima can be utilized to identify the ROI inside the tube. Anyway the tube vibrates, so the borders oscillate in the acquired image, and this may significantly effects the identification of the ROI (Fig. 6). For this, the first step in the algorithm is to split the acquired image in sub-image of size STEP lines, and to apply the search of the minima for the ROI identification to each of these sub-image.

The algorithm (Fig. 7), starting from the center of the tube, search on the left and right part of the tube the minimum values of the intensity and their column numbers. If such values are below an experimental determined threshold (indicating that the minimum identify a border and is not instead a local minimum due to noise or other effects), the algorithm searches for the outer and inner borders of the tube, that are determined as the first value of the column y for which the intensity is greater than the mean Intensity of the sub-image (outer border), or greater than the mean intensity of the sub-image minus a threshold (because, as from Fig. 5-b, the intensity inside the tube is lower than the intensity outside the tube). The inner borders of the tube are useful for the identification of ROI, while the outer borders of the tube are useful for deriving the tube caliber, for diagnostic purposes.

3.3.2. Defects detection and classification. Discard decision.

Once the ROI is identified, a Gaussian filtering is applied to reduce noise, and the Canny edge detector [31] is applied to the ROI to identify all the defects. Fig. 8 shows some examples of defects present in glass tubes (air lines and impurities).
The output of the Canny edge detector is a black and white image (Fig. 9 on the right). Air bubbles, knots, impurities and other defects are connected features in the images, but we also apply to the post canny images two dilations to fill-in gaps in the contours. Fig. 9 shows on the left two air lines, and on the right the related output from the Canny edge detector, with edge contours enclosed in rectangles.
After the applying of Canny, the edges (outer) contours in the images are identified and stored into a linked list in which only the end points of segments are stored (a rectangle would be stored as four points) [32]. The algorithm utilized is the one described in [33].

Defects, in particular air lines, can span across two or more images (Fig. 10-a), and for this reason we developed an algorithm that unifies contours (defects) across images. With references to Fig. 10-a and the simplified representation in Fig. 10-b, the algorithm check for contours in Image1 that have ends points with X=height and take such end points (A and M in Fig. 10-b). Then check In image 2 for contours that have ends points with X=0 and take such point (Σ, Ω). If condition (4) holds, the two contours are considered as the same contour.

$$Y\_A = Y\_\Sigma \ AND \ Y\_M = Y\_\Omega \qquad (4)$$

The two contours are now merged, and the resulting contour has the end points E, G, Y, X (Fig 10-c).

The three cameras inspect the continuous tube and are placed at the same distance from the Cutting and Discarding machine, so defects are allocated to a single cut tube knowing both the distance among cameras and the Cutting and Discarding machine and the tube speed. The three lists of defects coming from the three cameras are aggregated into a single list for each single tube. Each defect is enclosed in a bounding rectangle and the ratio length/width of the rectangle is used to differentiate between air lines and knots (impurities, inclusions).
The full set of defects in a single tube is used to decide whether that tube must be discarded or accepted. Quality requirements on tubes can change depending on the class of tubes and on their final usage, and plant supervisors can change these parameters dynamically through a Graphical User Interface or via a network link.

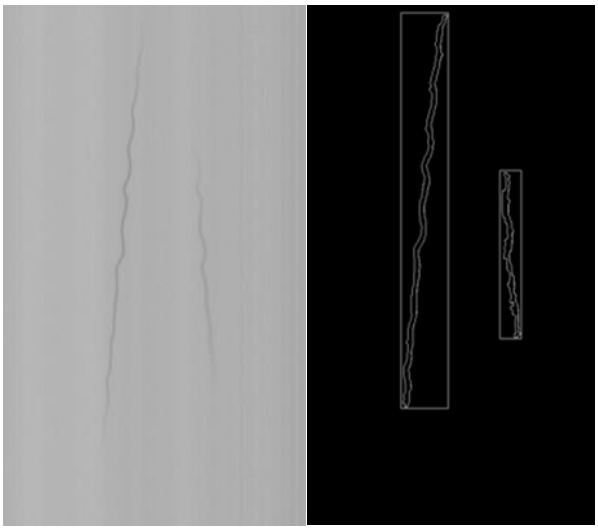

Figure 9. Two air lines identified in one camera. Raw image (on the left), and the same image after image analysis (on the right). The lines are straight, but due to the tube rotation they appear as curved, so the line length is due to the length of the bounding rectangle.

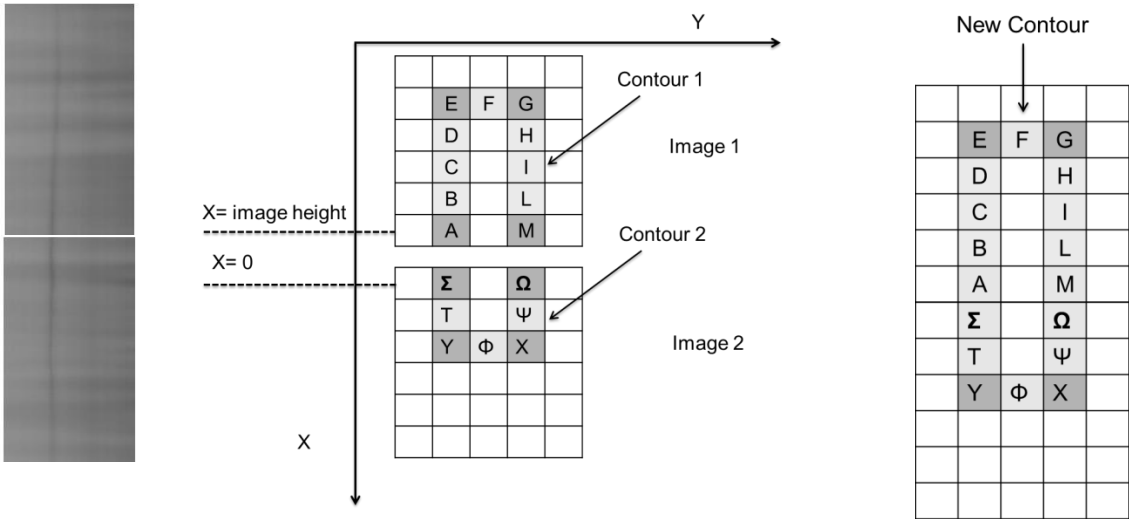

(a) (b) (c)

Figure 10: (a) is a single defect that is present in two acquired images. (b) after contour elaboration, two contours are identified: Contour 1 in Image 1, with end points A, E, G, H, and Contour 2 in Image 2, with end points Σ, Y, X, Ω. (c) After contours union, the New Contour is represented by points E, G, Y, X

3.4. Deployed software architecture

The overall inspection application is divided in 6 processes: one watchdog process starts and monitors the others, three processes (Camera_process), one for each camera, perform image analyses, one process manages the user interface (such GUI has been developed to limit the cognitive effort of operators [34], [35], [36], [37]), and one process (Discard_process) takes discard decisions and manages the I/O communications to the Cutting and Discarding Machine, Fig. 11. The three processes of cameras and the Discard_Process have higher priority. When one of the three Matrox frame grabbers receives 1000 line scans and a new image is ready, the image is stored in a circular buffer local to a camera process, and passed to a hook function, that contains the image analysis code to be executed on the image. The steps of saving an image in a circular buffer and invoking a hook function is done through the mDigProcess() function, provided by the Matrox MIL library (Fig. 11).

The three camera-related processes run concurrently. The hook function invokes all image

analyses routines (ROI identification, edge detection, contours extraction, defects identification and defects timestamping), and its results are stored in a memory mapped file that is accessible to all three camera-related processes and also to the Discard_process. The memory mapped file contains another circular buffer. Each one of the three concurrent camera-related processes writes in precise areas of the memory mapped circular buffer, so that each camera related process does not write in memory mapped areas written by the other two (scheme in Fig. 11). Following the timestamps of each defect, defects are allocated to the specific tubes, as tube speed and distance of cameras from cutting actuator are known. The Discard_process has access as well to the memory mapped file and the circular buffer with the defects and related timestamps. The number and the features of detected defects in each single tube are compared with the quality production requirements, and if the requirements are not met the Discard_process issues a relative command to the discarding actuator. Besides, a logging process, not shown in Figure 11, saves the list of defects and the discarding decision for each tube, and, on request, can saves the tubes images on disk for further analyses. The system runs on a four-core CMP [38]; each camera process is managed by a specific core, and core affinity [39] is ensured to minimize performance interferences at process swaps.
The system is controllable through a Graphical User Interface, that continuously shows the tubes, highlighting detected defects and stats related to the defects.

4 Assessment of the achieved quality

The inspection performances of the vision system have been evaluated in a glass tube foundry. All the tubes checked by the machine have been stored and analyzed off-line by expert operators to discover all the defects in the tubes. The inspection performed by humans is the best benchmark we had to measure the performance of our vision system, similarly to what has been done in other works [17], [19], [20], [40]. In our case, experts, working off-line in a laboratory, look at single tubes on a black background with an orthogonal white fluorescent light that highlights even the smallest impurities, and can inspect a suspect defect multiple times.

We measured the performances of the inspection vision system collecting a large number of tubes with different calibers, and we calculated the following quantities: Tubes Accepted (TA) by the vision system, Tubes Discarded (TD) by the vision system, Tubes Validated (TV) by operators actually meeting the quality requirements, Tubes Invalidated (TI) not meeting the quality requirements, tubes False positives (Fp) discarded by the system but meeting quality requirements and tubes False negatives (Fn) accepted by the system but not meeting the requirements. Following this naming, we categorized misclassifications among false positives *-alpha*, and false negatives *–beta*, according to the following formulas [40]:

$$alpha=Fp/(TA-Fn+Fp) \quad (5)$$
$$beta=Fn/(TD-Fp+Fn) \quad (6)$$

Our methodology consists in running the inspection with a quality requirement, and verify whether the machine accepts and discards correctly the single tubes as the expert human operators. In particular, we perform a stress test (M1), with quality requirements of no air lines longer than 10 mm and no knots bigger than 1 mm^2. Such condition represents limits conditions with respect to typical working parameters of the system. Table 1 shows that the inspection system provides low values for alpha and beta, and these values have been considered as being at state-of-art by experts of tube quality. In normal operation requirements (lines longer than 20mm), alpha and beta values are near 0.

By experimental tests, the errors that generate the alpha and beta values are concentrated in lines with length between 10 mm and 20 mm and knots between 1 mm^2 and 1.5 mm^2. To quantify the ability of the system to identify defects of such sizes, we perform a second test, M2, where 100 tubes with defects in the previous class were analyzed both by the inspection system both by the experts. The results of the M2 test are reported in table 2. The table presents i) the caliber of the tube, with outer diameter and thickness, ii) the percentage of air lines identified when compared with the air lines reported by expert operators, iii) the percentage of the cumulative air lines length calculated compared with the cumulative length observed by expert operators, iv) the air lines reported by the vision system but not observed by the operators (false air lines), v) the percentage of knots identified by the inspection system, vi) the percentage of knots classified by the system as air lines while experts considered them knots (false knots).

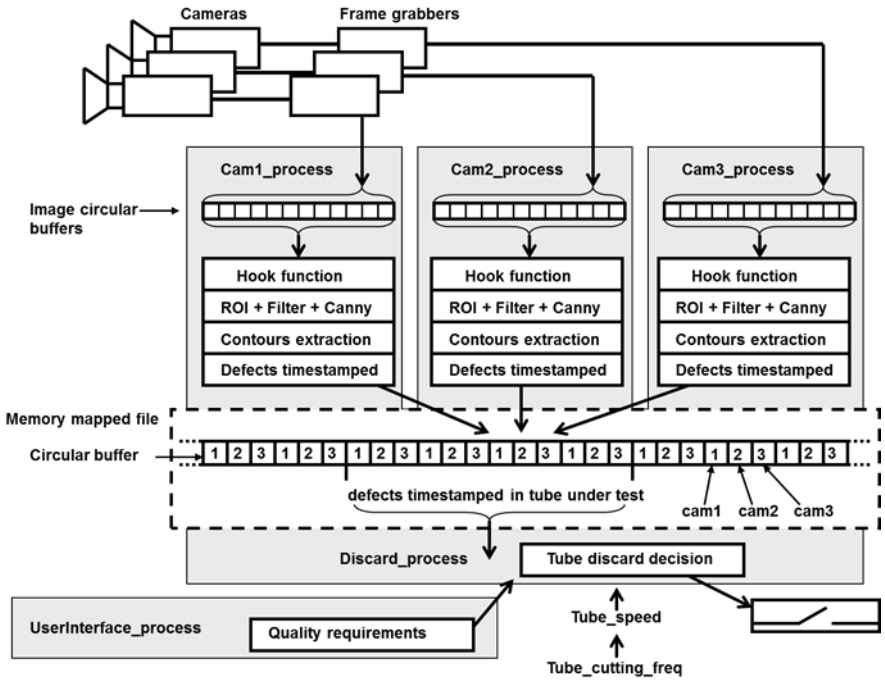

Figure 11: The processes involved in images analyses;
the Discard process reads all defects and decides tubes acceptances.

caliber (mm)	# tubes	accept. (TA)	discard. (TD)	valid (TV)	invalid (TI)	false pos. (Fp)	false neg. (Fn)	alpha	beta
8.65/.9	175	138	37	140	35	5	3	0.04	0.09
11.6/.9	210	181	29	180	30	3	4	0.02	0.13

Table 1. Two runs of tubes acceptance stress tests (M1), with percentages of false positives (*alpha*) and false negatives (*beta*).

caliber (mm)	air lines identified	Cum. air lines length calculated	false air lines	knots	false knots (air lines)
17.75/.6	88%	82%	10%	94%	6%
10.75/.5	85%	84%	11%	95%	5%

Table 2. Two runs of small defects identification test (M2), with percentages of true and false (nonexistent) defects. 100 tubes were used in this experiment.

Results indicate that the inspection system is less able to identify defects of small size. Anyway, such defects have no impact on the final quality of the tubes. In conclusion, the system is able to identify defects that generate quality issues at the state of the art of the actual requirements.

5 Conclusions

We described a vision-based inspection system for glass tubes that will be converted into vials, carpules or syringes. In this domain, pharmaceutical products have been recalled because of problems in the glass containers, so glass tube manufacturers are being demanded by pharmaceutical companies to improve

the quality of their products to prevent problems in the later steps of the production.
The described quality control system is based on three line-scan cameras and three LED linear illuminators, while a quad-core system performs the images analysis, and controls a cutting machine according to the detected defects. The quad core also interfaces with the cutting machine to derive the cutting frequency and derive tube speed, being tube speed necessary to derive the real sizes of the defects. Human operators can modify the quality requirements of glass tubes to be accepted at run time, through a Graphical User Interface or a network link.

The presented system proved effective in identifying defects and impurities in the order of tens of microns and was tested in a glass foundry and installed and working on two production lines. In particular, the inspection system misclassification rate is within the range $0.09 \div 0.13$, when working with stressing quality requirements.

Although the proposed system adopts a common approach for vision systems, specific problems induced by the production process have been solved, both at hardware and at software level. Having to inspect an object vibrating significantly, the adoption of a highly uniform illumination has simplified the feature extraction algorithms. The vibrations and rotations in the object also did not allow to compensate scarce illumination due to short exposure times and high magnifications via software, so we adopted a powerful illuminator at state of the art, while at software level we segmented acquired images and apply a local minima search algorithm. The need to inspect the tube at 360° was solved with a multi-camera system; as the tube flows continually, we develop specific algorithms to identify defect that span over multiple images, also produced by different cameras. Besides, we utilize circular buffers and synchronizations to manage the parallelism issues in the data coming from the cameras.
Future works will investigate techniques to improve small defects length detection, based on the analysis of their shape or by adopting different noise reduction techniques [41], and whether optimized architectures [42] can be utilized to reduce execution time or power consumption of such kind of workload. Besides, we will investigate the opportunity of introducing IEC 61131/IEC 61499 based techniques to model all the process plant [43].

References:

[1] Berry H.. Pharmaceutical aspects of glass and rubber; J. of Pharmacy and Pharmacology, v.5(11):1008-1023; Wiley, 2011.
[2] Sacha G.A., et al. Practical fundamentals of glass, rubber, and plastic sterile packaging systems, Pharmaceutical development and technology, v.15(1):6-34, 2010.
[3] Reynolds G. and Paskiet D.. Glass delamination and breakage, new answers for a growing problem; BioProcess International 9(11):52-57, 2011.
[4] Ennis R., Pritchard R., et al. Glass vials for small volume parenterals: Influence of drug and manufacturing processes on glass delamination. Pharmaceutical development and technology, v.6(3):393–405, 2001.
[5] Iacocca R.G. and Allgeier M.. Corrosive attack of glass by a pharmaceutical compound. Jou. of Material sciences, 42(3):801–811, 2007.
[6] Schwarzenbach M.S., et al. Topological structure and chemical composition of inner surfaces of borosilicate vials. PDA J. of Pharmaceutical science and Technology, v.58(3):169–175, 2004.
[7] Guadagnino E. and Zuccato D.. Delamination propensity of pharmaceutical Glass containers by accelerated testing with different extraction media; PDA Journal of Pharmaceutical science and technology, v.66(2):116-125, 2011.
[8] Iacocca R.G., Toltl N., et al.. Factors Affecting the Chemical Durability of Glass Used in the Pharmaceutical Industry. AAPS PharmSciTech, v.11(3):1340-1349, 2010.
[9] Bee J.S., et al. Effects of surfaces and leachables on the stability of bio-pharmaceuticals. Journal of Pharmaceutical Sciences, V.100(10):4158–4170, 2011.
[10] DeGrazio and Paskiet. The glass quandary; Contract Pharma, Jan./Feb. 2012
[11] Breakage and particle problems in glass vials and syringes spurring industry interest in plastics; IPQ In the News, August 7, 2011.
[12] Peng, Xiangqian, et al. An online defects inspection method for float glass fabrication based on machine vision. The International Journal of Advanced Manufacturing Technology 39.11-12 (2008): 1180-1189.
[13] Bechini, A. et al, Use of a CORBA/RMI Gateway: Characterization of Communication Overhead, Int. Work. on Software and Performance, Roma, Italy, June 2002
[14] O'Leary P.. Machine vision for feedback control in a steel rolling mill; Computers in Industry, v.56:997-1004, Elsevier, 2005.

[15] Jiang B.C., Jiang S.J., Machine vision based inspection of oil seals; Journal of Manufacturing Systems, v.17(3):159-166; Elsevier, 1998.
[16] Pham D.T., Jennings N.R. and Ross, I.. Intelligent visual inspection of valve-stem seals; Control engineering practice, v.3(9):1237-1245, Elsevier, 1995.
[17] Campoy P., Canaval J. and Pena D.. InsPulp-I©: an on-line visual inspection system for the pulp industry. Computers in Industry, v.56:935-942, Elsevier, 2005.
[18] Pham D.T., et al. Optimising neural networks for identification of wood defects using the bees algorithm; IEEE Int. conf. on industrial informatics, pp.:1346-1351, 2006.
[19] Cho C.S., Chung B.M. and Park M.K., 2005. Development of real-time vision-based fabric inspection system; IEEE Trans. on Industrial Electronics, v.52(4):1073-1079.
[20] Sari-Sarraf H. and Goddard J.S., 1999. Vision system for on-loom fabric inspection; IEEE Trans. on ind. applications, 35(6):1252-1259.
[21] Lahajnar F., et al. Machine vision system for inspecting electric plates; Computers in Industry, v.47:113-122, Elsevier, 2002.
[22] Laizola, Eskarne, et al. Computer-vision-based gob inspection system for monitoring and control in the glass industry. Electronic Imaging 2003. Inter. Society for Optics and Photonics, 2003.
[23] Boukouvalasa C., De Natale F., et al., ASSIST: automatic system for surface inspection and sorting of tiles; J. of Materials Processing Technology, v.82(1-3):179-188, Elsevier, 1998.
[24] King W.E., et al. Using MORPH in an industrial machine vision system. IEEE Symp. on FPGAs for custom computing machines, pp.:18-26, 1996, IEEE.
[25] Changyong Li, Qixin Cao, and Feng Guo. 2009. A method for color classification of fruits based on machine vision. *WSEAS Transactions on Systems* 8, 2 (February 2009), 312-321.
[26] Ivo Stancic, et al. Computer vision system for human anthropometric parameters estimation. WSEAS Transactions on Systems 8, 3 (March 2009), 430-439.
[27] Shang, Hui-Chao, et al. Online auto-detection method and system of presswork quality. Inter. Journal of Advanced Manufacturing Technology 33.7-8 (2007): 756-765.
[28] Adamo, F., et al. "A low-cost inspection system for online defects assessment in satin glass." Measurement 42.9 (2009): 1304-1311.
[29] Kumar, A.. Computer-vision-based fabric defect detection: a survey. IEEE Trans. Industrial Electronics, 55.1 (2008) 348-363.
[30] Pernkopfa F. and O'Leary, P. Image acquisition techniques for automatic visual inspection of metallic surfaces; NDT & E International, v.36(8):609–617, 2003.
[31] Canny J.. A computational approach to edge detection, IEEE Trans. Pattern Analysis and Machine Intelligence, 8(6):679–698, 1986.
[32] Bradski, Gary, and Adrian Kaehler. Learning OpenCV: Computer vision with the OpenCV library. O'Reilly Media, Inc., 2008.
[33] Suzuki, S. and Abe, K., *Topological Structural Analysis of Digitized Binary Images by Border Following*. CVGIP 30 1, pp 32-46 (1985).
[34] Shneiderman, S. B., & Plaisant, C. 2005. Designing the user interface 4 th edition. ed: Pearson Addison Wesley, USA.
[35] Dini, G., Foglia, P., Prete, C. A., & Zanda, M. (2014). Social and Q&A interfaces for app download. Information Processing & Management, 50(4), 584-598.
[36] Haapalainen E., Kim S.J., et al, 2010. Psycho-physiological measures for assessing cognitive load. 12th ACM Int. Conf. on Ubiquitous Computing, pp. 301-310.
[37] G. Dini, et al., A Social-Feedback Enriched Interface for Software Download, Journal of Organizational and End User Computing, 25(1), pp. 24-42, January-March 2013.
[38] P. Foglia, M. Solinas, Exploiting Replication to Improve Performances of NUCA-Based CMP Systems, ACM Trans. on Emb. Computing Systems, Vol. 13(3s), Art. 117, March 2014.
[39] Foglia P. et al. Reducing Coherence Overhead and Boosting Performance of High-End SMP Multiprocessors Running a DSS Workload. Journal of Parallel and Distributed Computing, V.65(3):289-306, 2005.
[40] Li, D., et al. Defect inspection and extraction of the mobile phone cover glass based on the principal components analysis. Intern. Journal Advanced Manuf. Technology, 1-10, 2014.
[41] Mary, D., et al. "Wavelets and Ridgelets for Biomedical Image Denoising. WSEAS Trans. on Systems 12, 3 (2013): 165-178.
[42] A. Bardine, et al, WayAdaptable D-Nuca Caches. Inter. Journals of High Performance Systems Architecture, Vol. 2, Issue 3/4, pp. 215-228, August 2010.
[43] Campanelli, S. et al. Integration of existing IEC 61131-3 systems in an IEC 61499 distributed solution. IEEE Emerging Technologies & Factory Automation Conf., pp.1-8, Sept. 2012.